

## **GPR SYSTEM PERFORMANCE COMPLIANCE ACCORDING TO COST ACTION TU1208 GUIDELINES**

LARA PAJEWSKI<sup>1</sup> (CORRESPONDING AUTHOR), MILAN VRTUNSKI<sup>2</sup>, ŽELJKO  
BUGARINOVIĆ<sup>2</sup>, ALEKSANDAR RISTIĆ<sup>2</sup>, MIRO GOVEDARICA<sup>2</sup>, AUDREY VAN DER  
WIELEN<sup>3</sup>, COLETTE GRÉGOIRE<sup>3</sup>, CARL VAN GEEM<sup>3</sup>, XAVIER DÉROBERT<sup>4</sup>,  
VLADISLAV BORECKY<sup>5</sup>, SALIH SERKAN ARTAGAN<sup>6</sup>, SIMONA FONTUL<sup>7</sup>,  
VÂNIA MARECOS<sup>7</sup> & SÉBASTIEN LAMBOT<sup>8</sup>

<sup>1</sup> DEPARTMENT OF INFORMATION ENGINEERING, ELECTRONICS AND TELECOMMUNICATIONS,  
SAPIENZA UNIVERSITY OF ROME, ROME, ITALY - LARA.PAJEWSKI@UNIROMA1.IT

<sup>2</sup> FACULTY OF TECHNICAL SCIENCES, UNIVERSITY OF NOVI SAD, NOVI SAD, SERBIA -  
MILANV@UNS.AC.RS, ZELJKO91BUG@GMAIL.COM, ARISTIC@UNS.AC.RS, MIRO@UNS.AC.RS

<sup>3</sup> BELGIAN ROAD RESEARCH CENTRE (BRRC), BRUSSELS, BELGIUM -  
A.VANDERWIELEN@BRRC.BE, C.GREGOIRE@BRRC.BE, C.VANGEEM@BRRC.BE

<sup>4</sup> INSTITUT FRANÇAIS DES SCIENCES ET TECHNOLOGIES DES TRANSPORTS, DE L'AMÉNAGEMENT ET  
DES RÉSEAUX (IFSTTAR), NANTES, FRANCE - XAVIER.DEROBERT@IFSTTAR.FR

<sup>5</sup> UNIVERSITY OF PARDUBICE, PARDUBICE, CZECH REPUBLIC - VLADISLAV.BORECKY@UPCE.CZ

<sup>6</sup> ANADOLU UNIVERSITY, TURKEY - SSARTAGAN@ANADOLU.EDU.TR

<sup>7</sup> NATIONAL LABORATORY OF CIVIL ENGINEERING (LNEC), LISBON, PORTUGAL -  
SIMONA@LNEC.PT, VMARECOS@GMAIL.COM

<sup>8</sup> EARTH AND LIFE INSTITUTE, UNIVERSITÉ CATHOLIQUE DE LOUVAIN,  
LOUVAIN-LA-NEUVE, BELGIUM - SEBASTIEN.LAMBOT@UCLouvain.BE

### **ABSTRACT**

*Ground Penetrating Radar (GPR) systems shall be periodically calibrated and their performance verified, in accordance with the recommendations and specifications of the manufacturer. Nevertheless, most GPR owners in Europe employ their instrumentation for years without ever having it checked by the manufacturer, unless major flaws or problems become evident, according to the results of a survey carried out in the context of COST (European Cooperation in Science and Technology) Action TU1208 “Civil engineering applications of Ground Penetrating Radar.” The D6087–08 standard, emitted by the American Society for Testing Materials (ASTM International), describes four procedures for the calibration of GPR systems equipped with air-coupled antennas. After a critical analysis of those procedures, four improved tests were proposed by a team of Members of the COST Action TU1208, which can be carried out to evaluate the signal-to-noise ratio, short-term stability, linearity in the time axis, and long-term stability of the GPR signal. This paper includes a full description of the proposed tests and presents the results obtained by scientists from Belgium, Czech Republic, Portugal, and Serbia, who executed the tests on their GPR*

*systems. Overall, five pulsed control units and nine antennas were tested (five horn and four ground-coupled antennas, with central frequencies from 400 MHz to 1.8 GHz). While the performed measurements are not representative enough to establish absolute thresholds for the tests, they provide a valuable indication about values that one could obtain when testing GPR equipment, if the equipment is working reasonably well. Moreover, by periodically repeating the tests on the same equipment, it is possible to detect any significant shift from previously obtained values, which may imply that the GPR unit or antenna under test is not working in a normal or satisfactory manner. We also believe that executing the tests described in this paper is a useful exercise to gain awareness about the behaviour of a GPR system, its accuracy and limits, and how to best utilize it.*

**KEYWORDS:** Ground Penetrating Radar (GPR); Antennas; Calibration; System performance compliance; Signal-to-noise ratio; Signal stability; Signal linearity in the time axis.

## 1. INTRODUCTION

Early Ground Penetrating Radar (GPR) technology was relatively primitive, data presentation was complex and interpretation of results was a difficult task [1]. Over time, the GPR technology has improved in terms of sensitivity, functional form, ease of use and information presentation. Systems have become lighter, more portable and self-contained; efficient data processing algorithms have been developed, the interaction of electromagnetic waves with soil and targets is better understood, and there is a stronger awareness of GPR limitations [2]-[5]. As a consequence, the GPR technique is nowadays increasingly used in a wide range of applications and is considered as a safe and versatile method, which is capable to provide accurate and reliable information in a fast and efficient way [6]-[11]. GPR surveys are successfully conducted in various environments, under conditions that may sometimes change on a daily basis in the context of long surveys. Thanks to the continuing technology and methodology improvements, it is expected that GPR will further advance in the coming years.

High precision and reliability in GPR measurements obviously require systems with very high linearity and stability, generating very low levels of disturbances.

As is well known, the measurement accuracy is the closeness of agreement between the measured quantity value and the true quantity value of a measurand (e.g., the amplitude of the electric field as a

function of time, in the GPR case); the sensitivity is a relation between the indication of an instrument and the corresponding change in a quantity being measured. Ideally, the accuracy and sensitivity of a GPR should be constant over its full operating range; in practice, most measurements involve some changes in accuracy and sensitivity and this type of imperfection is referred as non-linearity of the equipment (which is often emphasized at the extremes of the expected operating range). Being aware of the linearity properties of a GPR and understanding their impact on the measured values significantly aids data interpretation and contributes to the effectiveness of a survey; if the equipment demonstrates non-linearity, it may be not properly calibrated in some portions of the operating range, or else some components may be worn, or the signal-to-noise ratio (SNR) may be too low.

Stability is the key to predictability: if the measuring process is changing over time, the ability to use the gathered data for the evaluation of electromagnetic and geometrical properties of media and targets is diminished, and so is the capacity to use GPR results in making decisions. Selectivity is defined as the instrument's insensitivity to changes in factors other than the actual measurand, for instance to environmental factors (humidity, pressure, temperature); an instrument with better selectivity guarantees a higher stability. There are many further factors that may introduce instability in a GPR system, such as internal and external electromagnetic noise, alterations of feeding voltage, antenna shielding problems, mechanical vibrations, variations of antenna matching due to permittivity and conductivity changes in the surveyed media, and more; additionally, as in all electronic devices, the GPR stability can worsen over time due to deterioration or ageing of system components.

Noise is the unwanted electromagnetic energy that interferes with the ability of the receiver to detect the useful signal. Noise is always present in the environment and is also generated within the GPR system. If the level of disturbances generated by the radar is low, the detection probability of small signals is enhanced [12]. The use of appropriate signal processing procedures can improve the SNR in GPR investigations [13]-[15].

To verify the performance compliance of GPR equipment, suitable stability, linearity and SNR tests should be carried out on a regular

basis and in a controlled environment, by following procedures that should be standardized. However, few recognized international standards exist in the area of GPR [16] and, to the best of our knowledge, the calibration topic is covered only within one of them, namely in the ASTM D6087 - 08(2015)e1 “Standard Test Method for Evaluating Asphalt-Covered Concrete Bridge Decks Using Ground Penetrating Radar” emitted by the American Society for Testing Materials (ASTM International) [17]; therein, four procedures for testing GPR systems equipped with air-coupled antennas are described. Moreover, reliable GPR manufacturers shall suggest calibration and verification procedures for the equipment they produce.

Besides the poor availability of standards in the field, the importance of periodically testing and calibrating GPR instrumentation is often underestimated in Europe, according to a survey conducted during the Third General Meeting of COST Action TU1208 “Civil engineering applications of Ground Penetrating Radar.” This event was held in London, United Kingdom, on 4-6 March 2015, and was attended by 90 participants from 29 countries, from academia and industry: in addition to the only GPR manufacturer participating in the meeting, just a researcher from France, a team of researchers from Belgium, and another researcher from Belgium claimed to have experience on testing the stability, linearity and SNR levels of GPR systems. In particular, the researcher from France stated that in the scientific network of the French Ministry of ecological and solidary transition (MTES), composed by the Institut Français des Sciences et Technologies des Transports, de l’Aménagement et des Réseaux (IFSTTAR, Nantes, France) and the Centre d’études et d’expertise pour les risques, la mobilité, l’environnement et l’aménagement (CEREMA, France), procedures similar to those described in [17] had been executed various times throughout the years, to test the equipment owned by the institute. The research team from Université catholique de Louvain (UCL, Louvain-la-Neuve, Belgium) reported about their studies on the topic, which were published in [18], [19] and are resumed in the following paragraphs. The researcher from the Belgian Road Research Centre (BRRC, Brussels, Belgium) communicated that she executed the procedures of [17] during her PhD thesis (see Appendix 5 of [20]); in particular, she tested a commercial 2.3 GHz ground-coupled antenna, which did not fulfill the thresholds set by the ASTM standard for the long term

stability and signal to noise ratio, namely because of the short-term noise in the acquired signal. Additionally, a Member from Spain reported about research activities performed in the University of Vigo by her colleagues [21], which are resumed in the following of this section, too.

In [18], the stability over time and repeatability of a frequency-domain and a time-domain GPR system were investigated. The frequency-domain GPR was a combination of a vector network analyser and an 800–5200 MHz horn antenna. The time-domain GPR was a commercial control unit with a 900 MHz bow-tie antenna. Both GPR systems were calibrated several times by performing measurements with the antennas at different heights over a perfect electric conductor (PEC) in the laboratory, as well as over a water layer. Further measurements were performed over a thin water layer and a relatively thick sandy soil layer, as validating media. The frequency-domain GPR turned out to be relatively stable, while the time-domain GPR presented a significant drift, which according to the authors can be accounted for using corrections based on the air direct-coupling waves. Inversions for the thin water layer and the sandy soil layer provided reliable results and showed a high degree of repeatability for both radar systems. Results presented in [18] also show that water- and PEC-based calibrations provide very similar results for the GPR calibration functions, with useful practical implications in case the calibration of a low-frequency antenna is necessary and when a sufficiently large metal plane is not available. Furthermore, the error on the calibration due to inaccurate antenna heights over PEC (or water) yields significant uncertainties on the inversion results for the horn antenna and smaller uncertainties for the bow-tie antenna.

In [19], the time drift of a time-domain GPR with a 900 MHz antenna was quantified over a certain time period (28 hours, non consecutive but in identical situation) and the maximum observed time drift was 0.0978 ns. As a second step of the study, the maximum time and amplitude drift were characterized in the frequency domain, via the calculation of a frequency-dependent ratio, to be multiplied by the original spectrum of the signal in order to illustrate the effects of the drift. Third step of the study was the quantification of the sensitivity of soil characterization (by full-wave inversion) in response to a drift: the overestimation of the dielectric permittivity reached 50% for low

dielectric permittivity values, whereas the maximum underestimation was 25% for high permittivity values, following a gradient. The error on the estimation of the electric conductivity turned out to be much higher, reaching an extreme of 105.4% for the lowest original values, with an average of 102.5%. These results show that the inaccuracy of recorded GPR data caused by drift phenomena, or more in general by the system instability, can be disastrous for an inverse problem solution.

In [21], several tests were carried out in order to evaluate the short-term and long-term amplitude and arrival-time stability of a time-domain commercial GPR working with three different ground-coupled antennas having central frequencies of 500, 800, and 1000 MHz. The tests were taken and further developed from [22], where procedures for the calibration of GPR equipment were presented; such procedures were in turn taken from a Texas Department of Transportation report [23]. Actually, in [23] eight procedures to test the performance of GPR systems were proposed. Four of them are based on the evaluation of the GPR reflection from a large metal plate and allow measuring the noise-to-signal ratio, the short-term signal stability, the amplitude of the so-called ‘end reflection’ directly preceding the metal plate reflection (caused by impedance mismatch at the end of the antenna, according to [23]), and the variations in the time-calibration factor; another procedure makes use of a non-reinforced concrete slab placed on top of a metal plate and aims at measuring the signal penetration in concrete; one more procedure, with the antenna pointed directly up into the air, is to measure an “end reflection waveform” (superimposed on every waveform collected by the system, according to [23]). Finally, two procedures allow compensating the bouncing effects of air-coupled antennas mounted on vehicles and evaluating the influence of vehicle speed on GPR amplitudes.

Coming back to [21], inspiration concerning the warm-up time before executing the tests was taken from [24] and the obtained data were used to determine some parameters proposed in [25], as well. The results of [21] show that, after a warm-up time of about 10 minutes, the GPR system under test had high arrival time stability, ensuring correct positioning of the recorded reflections in time. On the other hand, the amplitude stability was not satisfactory; for practical purposes, amplitude instability may cause significant errors in the estimation of the electromagnetic properties of media (for example, when applying the

procedures customarily used in road pavement investigations for the estimation of the electromagnetic properties of road layers, where the amplitude of the signal reflected by a particular layer is compared with the amplitude of the signal reflected by a metal plate). As suggested in [21], when accurate amplitude values are needed, it is safer to repeat static measurements several times and take an average of the received signals, in order to minimize the amplitude instability effects. All stability tests of [21] were carried out in air and repeated in distilled water; in the latter medium the amplitude stability was significantly improved, which suggests that the examined antennas work better when placed in contact with an absorbent medium having an impedance different than the air (as is expected for ground-coupled antennas).

Following the Third General Meeting, two Members of COST Action TU1208 from Italy and United Kingdom analysed the ASTM SNR test proposed in [17]. They considered a reduced Taylor's expansion up to the second order of the expressions of SNR bias and variance; and, they derived a formula for tuning the SNR threshold according to a fixed target value of the GPR signal stability [26]. Moreover, they executed the SNR test of [17] on a time-domain commercial GPR equipped with three different horn antennas produced by the same manufacturer, having central frequencies of 1 GHz, 2 GHz, and again 2 GHz, to investigate the effects of the antenna frequency on the SNR [26]. While the authors of the present paper appreciate the valuable efforts done in [26], it is the opinion of the authors that the SNR test of [17] is inherently not correct, for reasons explained in Sub-section 2.1 of the present paper.

Before introducing and describing the content of the present paper, a few more studies available in the GPR literature are worth being mentioned.

Various scientific-technical reports from the United States can be found on the web, where the tests proposed in [17], [21] and [23] are suggested; the report [27] is especially interesting and includes, in Appendix B, the description of almost all tests of [21] and [23], plus a procedure for evaluating the metal plate reflection symmetry. In [28] it was recommended to calibrate GPR systems at least once per year, based on the results of the tests described in [27].

In [29], the authors assessed the accuracy of GPR evaluations of propagation velocity and two-way travel time. By using time picks from

a common midpoint radargram recorded by a GPR equipped with a 200 MHz antenna, confidence limits of the order of 0.01 m/ns were found for velocity estimates; the confidence limits for two-way travel time estimates were of the order of 1 ns. In [30], the velocity inaccuracy level found in [29] was translated to an uncertainty of 12% in the estimated moisture content of a typical soil.

In the recently published paper [31], a new method for the stability evaluation of GPR systems was proposed, based on statistics. Four sets of experiments were carried out in an anechoic chamber and on a sandbox, to compare the stability performances of a commercial impulse GPR system with a 900 MHz ground-coupled antenna and a stepped-frequency GPR system covering the 50 MHz – 4 GHz range, based on a vector network analyser equipped with a pair of homemade bow-tie antennas. The influence of the warm-up time, environmental noise and antenna vibration on the GPR signal instability was investigated. In agreement with [18], it was found that the GPR signal recorded by the stepped-frequency GPR system was more stable than the impulse GPR system (at a cost of a longer sweep time, hence a slower survey speed). A warm-up time of several minutes turned out to be enough for the impulse system, whereas the stepped-frequency system needed no warm-up time (but only because it was warmed up before the measurement, to perform a standard calibration of the vector network analyser and coaxial cable). Environmental noise was found to have a negligible influence on the stability performance of the impulse system, probably because – in normal conditions – the environmental noise is much weaker than the instantaneous electromagnetic power radiated by a GPR. Mechanical vibrations, instead, were found to have a severe impact on the GPR stability (in agreement with [27]): the instability index was increased by more than one order of magnitude in a vibrating condition, compared to a static condition; it is therefore very important to undertake shock-proof measures when using a GPR mounted on a vehicle. Finally, the instability index evaluated by considering the direct wave, only, turned out to be similar to the instability index evaluated by considering the reflection from a metal plate; therefore, by using the index proposed in [31], a simple measurement of the direct signal seems to be enough for the evaluation of the instability of a GPR system (no need of using a metal plate). However, it is the opinion of the authors of the present paper that the

implementation of the test proposed in [31] may be too difficult for an average GPR user lacking of a scientific background; to make that text executable by everyone, the calculation of the instability index should be incorporated in the GPR system software, which should also assist the user in performing the test.

In this context, the international group of TU1208 Members authoring this paper focused on the standardised procedures described in [17] and critically analysed them. After a series of exploratory experiments carried out at the BRRC, with the aim of better understanding the merits and limits of the ASTM tests, in-depth discussions took place and four improved tests were defined as an output of the 2017 Working Group Meeting “Guidelines for the use of GPR in civil engineering” of COST Action TU1208, held at the COST Association premises in Brussels, Belgium, on 9-13 January 2017. In this paper, the four improved tests are presented (Section 2). They can be used to test GPR systems equipped with both air-coupled and ground-coupled antennas; and, they allow the quantitative experimental evaluation of the SNR (Sub-Section 2.1), signal stability over time (Sub-Section 2.2), signal linearity in the time axis (Sub-Section 2.3), and signal long-term stability (Sub-Section 2.4). During 2017, the four improved test were executed by research teams from Belgium (BRRC), Czech Republic (University of Pardubice, Pardubice), Portugal (National Laboratory of Civil Engineering, LNEC, Lisbon), and Serbia (Faculty of Technical Sciences of the University of Novi Sad, Novi Sad), to verify the performances of five commercial impulse GPR control units and nine commercial antennas with central frequencies ranging from 400 MHz to 1.8 GHz (five horn and four ground-coupled antennas); all the obtained results are reported and commented herein. The tests and experimental results were presented at the Final Conference of COST Action TU1208, held in Warsaw, Poland, on 25-27 September 2017 [32]; the results of measurements carried out in Serbia were also presented at the 2018 European Geosciences Union General Assembly (EGU GA), held in Vienna, Austria, on 8-13 April 2018, in the framework of the session “COST Actions in Geosciences: breakthrough ideas, research activities and results” [33].

The improved tests are being integrated in the guidelines for the use of GPR in civil engineering proposed by the COST Action TU1208. Given the afore-mentioned scarce availability of standards in the area of

GPR and having observed the existence of inhomogeneous recommendations and use practices in different countries, COST Action TU1208 worked hard on leveraging the gaps and yielded three guidelines for the use of GPR in some civil engineering tasks, plus a volume of recommendations for a safe geophysical prospecting [34]. The main focus of the three guidelines is on GPR road inspection, detection and localization of utilities in urban areas, and assessment of concrete structures (concrete bridges, tunnels and floors). As in all civil engineering applications of GPR it is very important to be aware of the stability, linearity and repeatability of the employed equipment, it was decided to include the four improved GPR performance compliance tests in the guidelines. Such guidelines are currently being refined and finalized, before being published in open access on the website of the Action ([www.gpradar.eu](http://www.gpradar.eu)).

We hope that the GPR performance compliance tests described in this paper will be executed by other research teams, private end-users and manufacturers, in the near future, on a wide variety of control units and antennas, on both brand new and older equipment; by sharing information about the obtained results, the GPR community can establish reasonable thresholds for the tests, which will help to distinguish between equipment working properly and flawed equipment (so that, in case of flawed equipment, the manufacturer can be contacted to check and possibly repair or calibrate the equipment). Our plans for future work also include investigating how the results of the proposed performance compliance tests translate into accuracy levels of measured physical and geometrical quantities, in various applications of the GPR technique.

## 2. TESTS

Four tests are proposed, which can be used to test GPR systems equipped with both air-coupled and ground-coupled antennas. They allow experimentally quantifying the SNR (Sub-Section 2.1), signal stability over time (Sub-Section 2.2), signal linearity in the time axis (Sub-Section 2.3), and signal long-term stability (Sub-Section 2.4). These tests can be carried out to assess the performance of a GPR system, in order to gain awareness about its accuracy and precision. They provide a baseline for evaluating the performance of new GPR equipment currently under development. It is also advised to

periodically repeat the tests on the same equipment, to monitor its performance over time and detect any significant shift from previously obtained values, which may imply that the GPR control unit or antenna under test is not working correctly. The tests proposed herein do not have the ambition to become compulsory; if the user guide of a GPR system includes tests proposed by the manufacturer, they take preference over the procedures described herein.

In all the proposed tests the antenna is placed at a certain height above a square metal plate, to enhance the amplitude of the reflected signal and guarantee repeatability of the test; in this configuration, a number of traces are recorded (see Figure 1, showing photos of the experimental setup used in Serbia and Portugal).

Common parameters for all tests are:

- Warm-up time:

Non negligible variations of results can occur during operation, if the GPR electronic components are not given the possibility to initially reach a temperature that provides the overall system with suitable stability and performance; based on experiments carried out by the authors, the warm-up time should be at least 30 minutes, or according to recommendations by the manufacturer.

- Metal plate size:

Depends on the central frequency of the antenna and is given by:

$$L = D + 2\sqrt{5}\lambda_c \quad (1)$$

where  $L$  is the minimum side length of the metal plate,  $D$  is the maximum aperture dimension (for aperture antennas, such as horns) or the maximum antenna dimension (for bow-tie and dipole antennas),  $\lambda_c = c/f_c$  is the wavelength at the central frequency of the spectrum emitted by the antenna, and  $c$  is the light velocity in the air. If the antenna size is not known, then a pejorative assumption of  $D$  can be made based on the size of the antenna box and any other useful available information about antenna geometry and position inside the box. A smaller metal plate may be used for tests presented in Sub-sections 2.2-2.4, although not recommended; Eq. (1) has to be strictly respected for the test presented in Sub-section 2.1 (unless information

about the antenna beam width is available, which can make it possible to use a smaller plate).



**FIG. 1** – **(a)** Experimental setup for a 400 MHz ground-coupled antenna in a laboratory of the Faculty of Technical Sciences, in the University of Novi Sad, in Serbia. **(b)** Experimental setup for 1 GHz and 1.8 GHz air-coupled antennas in a laboratory of the National Laboratory for Civil Engineering of Lisbon, in Portugal.

## 2.1 Signal-to-Noise Ratio (Test 1)

In this test two series of measurements are carried out, at two different distances between the metal plate and the antenna.

For the first series of measurements (see Figures 2(a) and Fig. 3):

- The distance between the metal plate and the antenna is  $h_1 = 2\lambda_c$ ;
- The time window (TW) is at least twice the two-way travel time from the antenna to the metal plate ( $TW > 8\lambda_c/c$ ).
- 100 waveforms are recorded.
- The average reflection amplitude  $\langle A_{mp} \rangle$ , that is the average peak-to-peak amplitude of the first echo coming from the metal plate, is evaluated.

In Figure 2(a), the sketch of the antenna is meant to represent the set of receiving and transmitting antennas (nowadays, they almost always are two distinct devices, which may be included in a common box or in two separate boxes). The distance  $h_1$  guarantees that the first reflection coming from the metal plate is well separated from the so-called direct wave (as illustrated in Figure 3), which is the pulse

travelling straight from the transmitting to receiving antenna (or, in horn antennas, the pulse reflected at the bottom of the antenna); this claim is

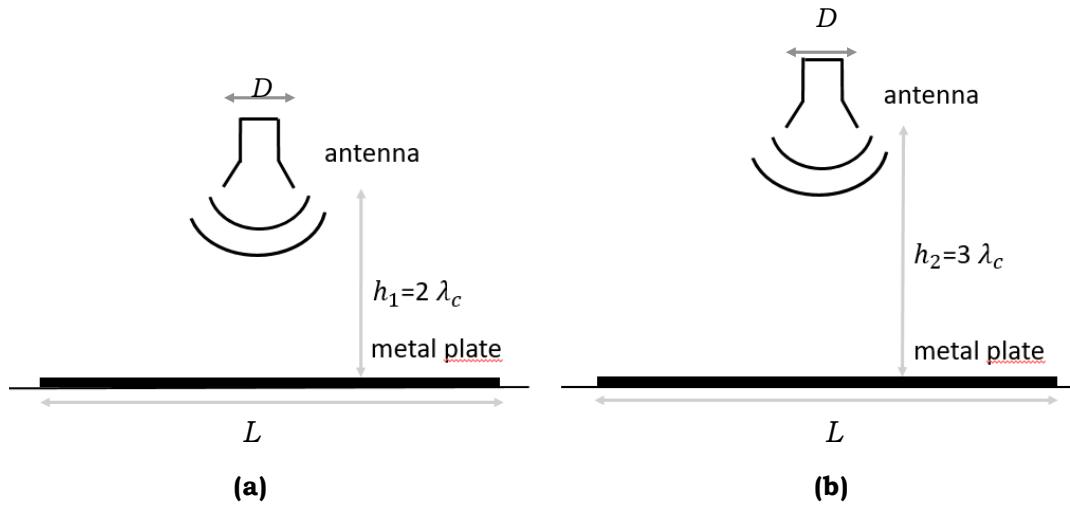


**FIG. 2** – Sketches of the experimental setup for Test 1: **(a)** Measurement series 1; **(b)** Measurement series 2.

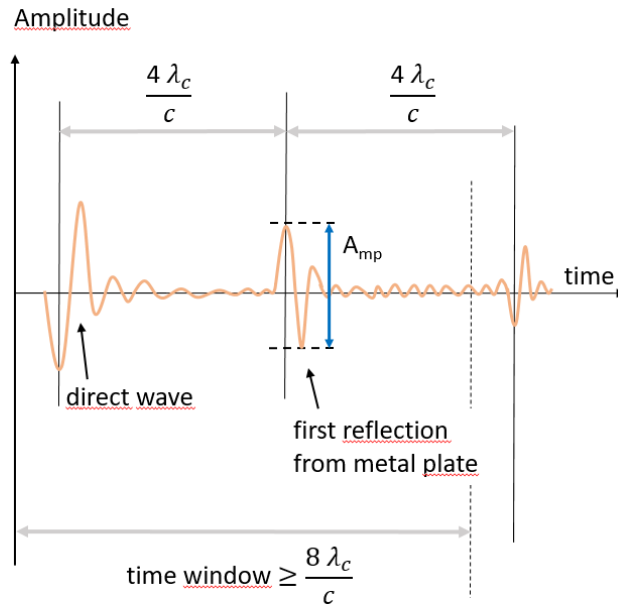


**FIG. 3** – Sketch of a GPR trace, to illustrate the choice of geometrical parameters, settings, and quantities to be evaluated, for measurement series 1 of Test 1.

based on the assumption that the pulse emitted by radar is  $2\lambda_c/c$  long (or shorter), as is customarily true for ultra wideband pulses popularly used in GPR.

For the second series of measurements (see Figures 2(b) and 4), the same GPR settings as in the first series are used and, again, 100 waveforms are recorded. The antenna height and the evaluated quantity are different:

- The distance between the metal plate and the antenna is  $h_2 = 3\lambda_c$ ;
- The suggested 'relevant time window' starts  $2\lambda_c/c$  after the absolute maximum amplitude of the signal, and is  $2\lambda_c/c$  long.
- The average amplitude  $\langle A_n \rangle$ , that is the average peak-to-peak noise amplitude over the 'relevant time window', is evaluated. Of course noise has an irregular time shape and does not appear as a series of pulses with peak-to-peak amplitudes, it is therefore proposed to evaluate  $A_n$  as the difference between the maximum and minimum amplitudes of noise over the considered 'relevant time window'.

An indicator of the signal-to-noise ratio can finally be calculated, by using the following formula:

$$I_{SNR} = \frac{\langle A_{mp} \rangle}{\langle A_n \rangle} \quad (2)$$

The higher this quantity, the better the quality of the signal is. In Section 3, examples of  $I_{SNR}$  values obtained by the authors are reported and commented on.

The suggested minimum  $L$  value, given by Eq. (1), is to make sure that any unwanted reflection coming from outside the metal plate is received after the metal plate echo when the antenna height is  $h_1$  and after the 'relevant time window' when the antenna height is  $h_2$ . Under the simplified assumption of geometrical optics (i.e., by describing the propagation of electromagnetic fields in terms of rays) and with reference to the scheme in Figure 5(a): if  $L = D + 2\sqrt{5}\lambda_c$ , the two-way travel time from A to B is  $6\lambda_c/c$ , which is equal to the two-way travel time from B to C plus the pulse time duration,  $4\lambda_c/c + 2\lambda_c/c$ ; this guarantees that reflections coming from outside the metal plate do not affect the results of measurement series 1. In Figure 5(b), the two-way travel time from A to B is  $2\sqrt{14}\lambda_c/c \approx 7,48\lambda_c/c$ , which is longer than  $6\lambda_c/c$ ; this guarantees that reflections coming from outside the metal plate do not affect the results of measurement series 2.

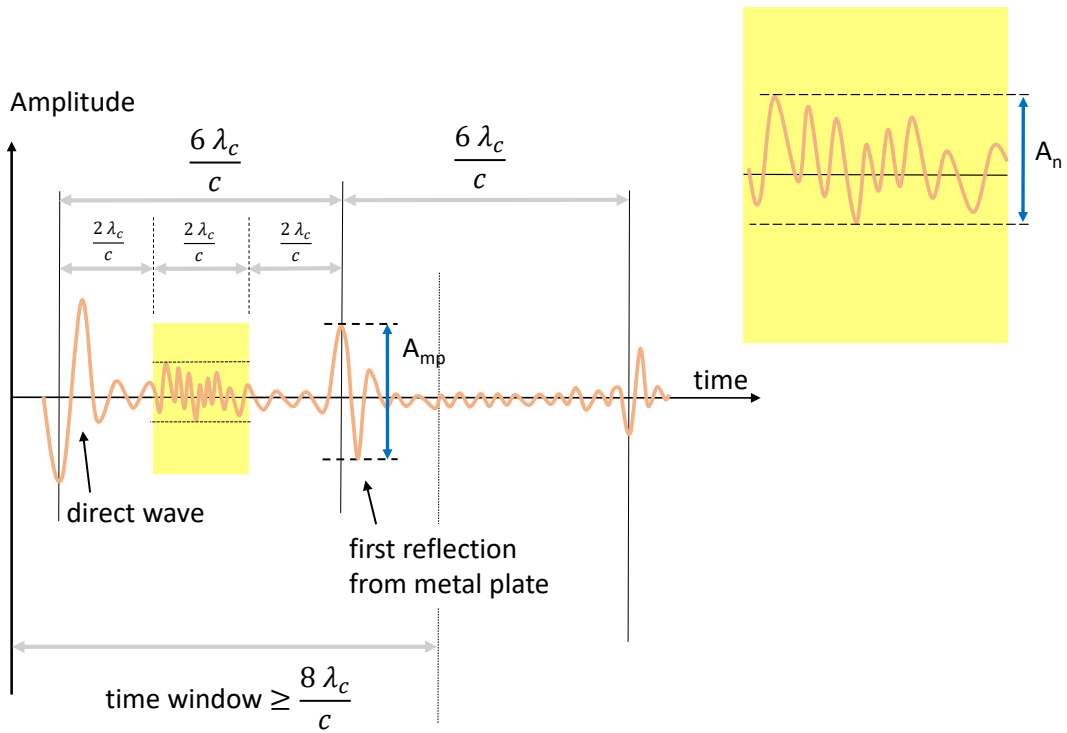


**FIG. 4** – Sketch of a GPR trace, to illustrate the choice of geometrical parameters, settings, and quantities to be evaluated, for measurement series 2 of Test 1.

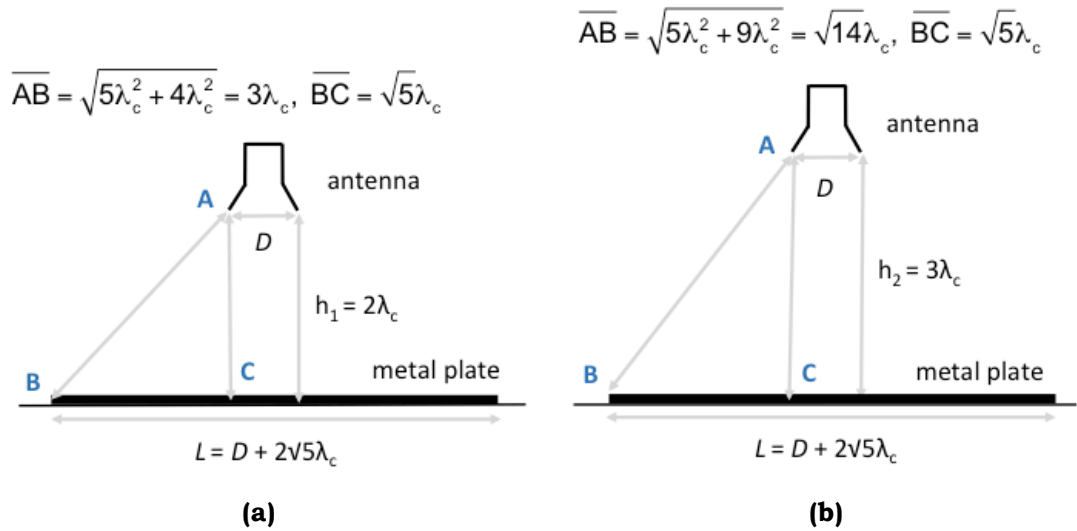


**FIG. 5** – Geometrical sketches to explain the choice of the metal plate size.

By using a larger metal plate, with  $L' = D + 2\sqrt{7}\lambda_c$ , both measurement series 1 and 2 could be performed with the antenna at  $h_2$  from the metal plate (the values of  $I_{SNR}$  would be obviously lower, because the peak-to-peak amplitude of the metal plate echo would be smaller, due to the longer propagation path). As an enlargement of the metal plate of  $L' - L \approx 0.82\lambda_c$  may be an issue at low frequencies, it was decided to propose a 'more complicated' test, with two separate series of measurements, in order to keep the metal plate as small as possible. Note also that, if information about the antenna beam width is available, it may be possible to reduce the metal plate size accordingly.

The main differences between Test 1 and the SNR test for air-launched antennas of [17] (paragraphs 6.2.1.1-6.2.1.3), as well as the authors' doubts about the validity of the test of [17], are now discussed.

In [17], it is recommended to position the antenna at a far field distance above a square metal plate, where the far field distance is defined as 'approximately equal to the maximum dimension of the antenna aperture ( $D$ )'; the recommended minimum side length of the metal plate is  $4D$ . The warm-up period is 20-min, or the time recommended by the manufacturer. After warming up the GPR, 100 waveforms are recorded. For each waveform, the signal-to-noise ratio is calculated as the ratio between the signal and noise levels; the signal level is defined as the amplitude of the echo from the metal plate, whereas the noise level is defined as the maximum amplitude occurring after the metal plate reflection and up to the 50% of the time window normally used with the antenna. Finally, the average signal-to-noise value of the 100 waveforms is calculated and taken as the signal-to-noise of the system. In [17], it is stated that this value should be greater than or equal to 20 (+26.0 dB).

A first doubt is concerned with the far field distance definition used in [17]. As is widely stated in the antenna literature, such definition is adequate for measuring the properties of antennas with  $D \leq \lambda_c$ , only, whereas for larger antennas the far field distance is generally taken as  $2D^2/\lambda_c$ . For pyramidal horns, which are popular air-launched solutions for GPR applications, a much longer distance than  $2D^2/\lambda_c$  may be necessary to measure the far field antenna properties, due to the large phase deviations across their apertures [35]. While the far field distance is not correctly defined in [17], the opinion of the authors is that the SNR is a quantity that can be measured in the near field, too,

therefore the inaccurate definition taken for the far field distance does not compromise the feasibility of the test. Nevertheless, at the suggested distance between the metal plate and the antenna, the first metal plate echo may arrive immediately after the direct wave if the pulse length is  $2\lambda_c/c$ ; in other words, unless the pulse emitted by the GPR is significantly shorter than  $2\lambda_c/c$ , the measured trace will consist of the direct wave immediately followed by a sequence of multiple metal plate reflections, with no possibility to measure noise levels in between the echoes. It is the opinion of the authors that this is one of the main faults of the SNR test of [17], which makes it inapplicable in most cases.

Another major problem of the SNR test of [17] is the indicated time interval for the measurement of the noise level. As already mentioned, the noise level is defined in [17] as the maximum amplitude after the first metal plate reflection, up to 50% of the time window normally used with the antenna. Provided that a ‘normally used time window’ is a questionable concept, because the time window depends on the survey objectives and on the electromagnetic properties of the investigated materials, it is highly probable that this procedure leads to mistake the maximum amplitude of the second reflection coming from the metal plate as the level of noise. For example, in [26] the SNR test of [17] was applied to a 1-GHz horn ( $\lambda_c = 30$  cm) and two 2-GHz horns ( $\lambda_c = 15$  cm). Each antenna was tested at three different distances from the metal plate:  $h_A = 30$  cm,  $h_B = 40$  cm and  $h_C = 50$  cm. Therefore, the two-way travel time from the antenna to the metal plate and back to the antenna was  $t_A = 2$  ns,  $t_B \approx 2.7$  ns and  $t_C \approx 3.3$  ns in the three cases, respectively. The time window was set to 25 ns for the 1-GHz horn and to 15 ns for the 2-GHz horns. The observation window for the evaluation of the noise level started after the first metal plate echo and ended at 12.5 ns for the 1-GHz horn, at 7.5 ns for the 2-GHz horns. Accordingly, the second reflection coming from the metal plate was always included in the noise level observation window.

It is not clear whether [17] suggests to measure the maximum absolute amplitude or the maximum peak-to-peak amplitude of signal and noise. It is also noticed that the warm up period suggested in [17] is shorter than the one proposed in this paper. Based on the results of the tests carried out by the authors, 20 min does not seem enough for many GPR systems to reach stability (see Sub-section 2.4); this is in agreement with the ASTM D4748 - 10(2015) “Standard Test Method for

Determining the Thickness of Bound Pavement Layers Using Short-Pulse Radar” [36], where it is advised to warm up the GPR system prior to a survey for a period recommended by the manufacturer, typically between 30 minutes and 1 hour (paragraph 8.2). Finally, although the SNR test of [17] is recommended for air-launched antennas, only, the (faulty) procedure seems applicable to ground-coupled antennas, too, once the practical problem of how to lift them is solved.

## 2.2 Signal Stability (Test 2)

To test the signal stability, the same test configuration as in Test 1 is used, with  $h_1$ . The time window is at least twice the two-way travel time from the antenna to the metal plate ( $TW > 8\lambda_c/c$ ) and 100 traces at the maximum data acquisition rate are recorded. An indicator of the signal stability can be calculated by using the following formula:

$$I_{stability} = (A_{MAX} - A_{min})/A_{avg} \quad (3)$$

where  $A_{MAX}$  is the maximum and  $A_{min}$  is the minimum peak-to-peak amplitude of the metal plate reflection, selected among all 100 recorded traces, and  $A_{avg}$  is the average peak-to-peak amplitude of the metal plate reflection. The smaller the quantity  $I_{stability}$ , the better is the stability of the system. In Section 3, examples of  $I_{stability}$  values obtained by the authors are reported and commented on.

The ASTM stability test is described in paragraphs 6.2.2.1-6.2.2.2 of [17]. The same test configuration as in the SNR ratio test is used; 100 traces are recorded at the maximum data acquisition rate and the signal stability is calculated by using an equation similar to Eq. (2), where  $A_{avg}$  is the average trace amplitude of all traces instead of the average peak-to-peak amplitude of the metal plate reflection.

As far as the experimental set-up and GPR settings are concerned, differences between the signal stability test proposed herein and the ASTM stability test were already discussed in Section 2.1. For this test, those differences are of minor importance because noise levels are not measured. In the ASTM stability test it is not clear whether absolute amplitudes or peak-to-peak amplitudes should be measured.

## 2.3 Linearity in the time axis (Test 3)

In Test 3, the same test configurations as in Test 1 are used. Additionally, measurements in a third configuration are carried out, with

$h_3 = 2.5 \lambda_c$  (see Figure 6). The time window is at least twice the two-way travel time from the antenna to the metal plate at the longest distance  $h_2$  ( $TW > 12\lambda_c/c$ ). A single waveform is recorded per configuration. For each configuration  $i$  ( $i = 1, 2, 3$ ), corresponding to  $h_i$ , the time delay  $\Delta t_i$  is determined: this is defined as the difference between the absolute maximum amplitude of the direct wave and the absolute maximum amplitude of the echo coming from the metal plate. The following absolute differences are then calculated:  $T_{21} = |\Delta t_2 - \Delta t_1|$ ;  $T_{31} = |\Delta t_3 - \Delta t_1|$ . The corresponding speed factors  $C_{21}$  and  $C_{31}$  are calculated as:

$$C_{21} = (h_2 - h_1)/T_{21} \quad (4)$$

$$C_{31} = (h_3 - h_1)/T_{31} \quad (5)$$

The relative variation in the measured speed can be finally evaluated, as follows:

$$Sv_{rel} = \frac{2|C_{21} - C_{31}|}{C_{21} + C_{31}} \quad (6)$$

The smaller the quantity  $Sv_{rel}$  the better is the linearity of the system in the time axis. In Section 3, examples of  $Sv_{rel}$  values obtained by the authors are reported and commented on.

While executing this test, a special attention must be paid to the accuracy of height measurements and the horizontality of the antennas: any error induces notable bias in the evaluation of  $Sv_{rel}$  (see the relevant discussion in Section 3).

The original ASTM linearity test is described in paragraphs 6.2.3.1-6.2.3.2 of [17]. The same test configuration as in the SNR ratio test is used, except that any reflecting object can replace the metal plate. Measurements are performed at three different distances between the antenna and reflector, which are defined as distances corresponding to 15%, 30% and 50% of the time window normally used with the system. The variation in time calibration factor is calculated with a formula similar to Eq. (6), without the modulus. Substantially, our test is the same as in [17], but the metal plate is used as reflector, and the three considered distances between the antenna and the reflector are different than in [17].

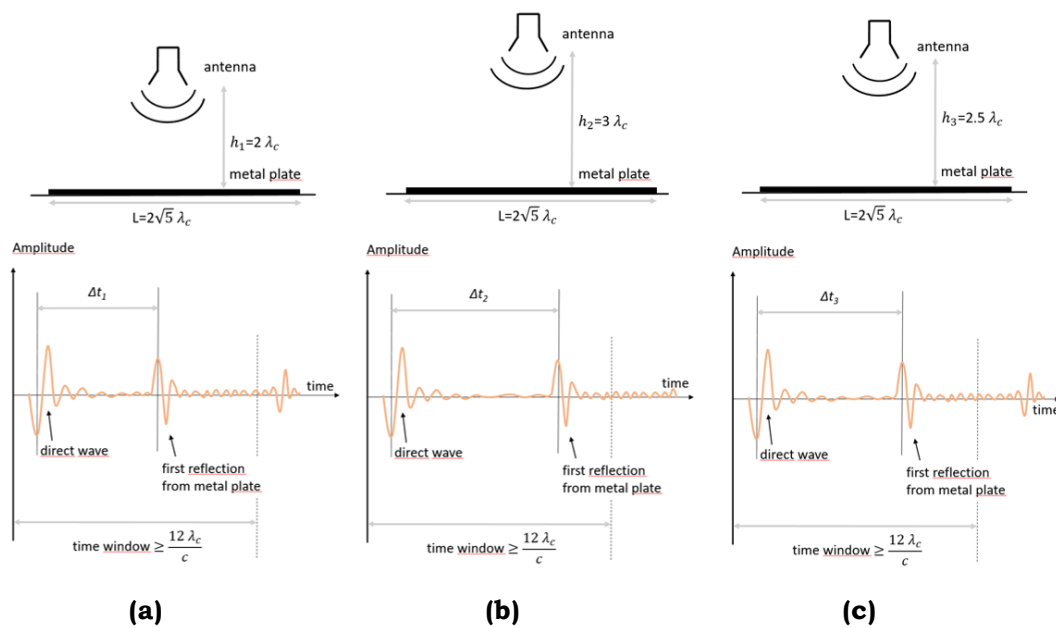


**FIG. 6** – Sketches of the experimental setup for Test 3, and GPR traces: **(a)** Measurement series 1; **(b)** Measurement series 2; **(c)** Measurement series 3.

#### 2.4 Long-term stability (Test 4)

In Test 4, the same test configuration as in Test 1 is used, with  $h_1$ . The time window is at least twice the two-way travel time from the antenna to the metal plate ( $TW > 8\lambda_c/c$ ). Every minute, for at least 120 minutes, 10 waveforms are recorded. Hence, at least 1200 traces are recorded in total, and it is even better if traces are recorded for a longer time (e.g., a time similar to the length of the longest surveys carried out with the equipment under test). For each waveform  $w$  ( $w = 1, \dots, T$ , being  $T$  the total number of traces) the peak-to-peak amplitude  $A_w$  of the metal plate first echo is determined. The sliding-average amplitudes  $M_q$  ( $q = 1, \dots, T - (N - 1)$ ) are then calculated, by using the following formula where the suggested value for  $N$  is 10:

$$M_q = \frac{1}{N} \sum_{j=0}^{N-1} A_{q+j} \quad (7)$$

The sliding-average amplitudes  $M_q$  are then plotted against time (or as a function of  $q$ ). Realizing such a graph helps to gain awareness about the behaviour over time of the GPR system at hand and allows discovering how long is the warm-up time needed by the system. An

example is presented in Figure 7 (data are from the BRRC): in this case, waveforms were recorded for 180 minutes; it can be observed that about 30 min of warming up are necessary, moreover a drift occurring after using the antenna for about 100 min can be noticed; Based on preliminary tests carried out by the BRRC, the long-term stability of GPR systems seems to be significantly affected by atmospheric conditions; however, more tests are necessary to confirm this remark.

The long-term stability factor  $LTStability$  is defined as the maximum between the following two quantities:

$$Q_1 = \frac{M_{MAX} - A_{1w}}{A_{1w}} \quad (8)$$

and

$$Q_2 = \frac{|M_{min} - A_{1w}|}{A_{1w}} \quad (9)$$

where  $M_{MAX}$  and  $M_{min}$  are the maximum and minimum values of the sliding-average amplitudes after the warm up and  $A_{1w}$  is the first (reference) trace after the warm up (note that  $A_{1w}$  might be replaced by  $M_1$  in Equations (8) and (9), i.e., it makes sense as well to consider the first sliding-average amplitude after the warm up as a reference, instead of  $A_{1w}$ ). The smaller the long-term stability factor, the better is the long-term stability of the system. In Section 3, examples of results obtained by the authors are reported and commented on.

The original ASTM long-term stability test is slightly different and is described in paragraph 6.2.4.1 of [17]. The same test configuration as in the SNR test is used. The GPR is allowed to operate for 120 minutes and a waveform every minute is recorded. The long-term stability factor is calculated as the difference between the largest amplitude of metal plate reflection measured between 20 and 120 minutes, and the amplitude measured after 20 minutes, normalized to the amplitude measured after 20 minutes. In the test proposed herein, the 20 minutes time is replaced by the warm-up time (which can change significantly among different systems), moreover a higher number of traces are recorded and the concept of sliding-average amplitudes is used, because usually amplitudes show large oscillations over a short time. The amplitude of those short-term variations can be estimated from the

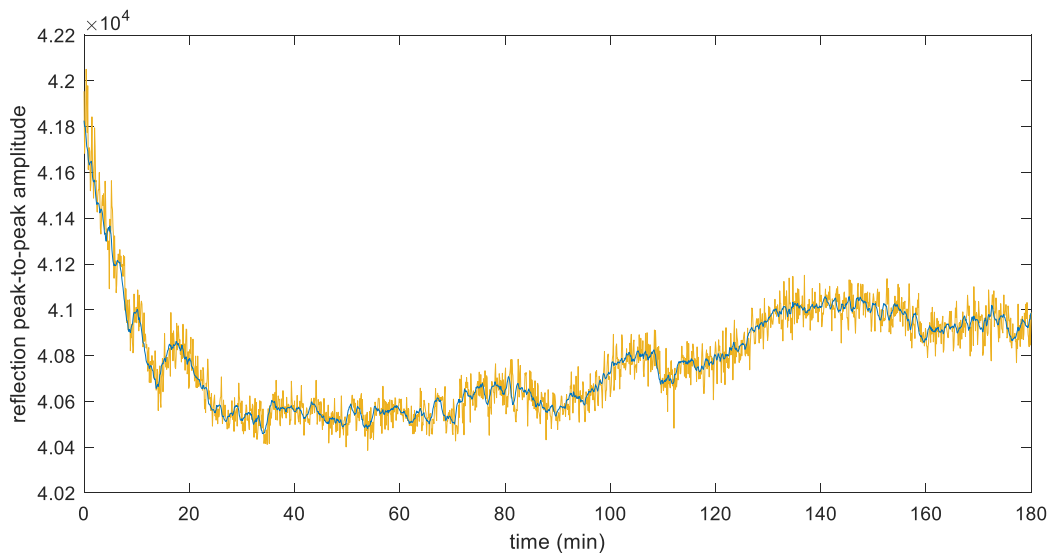


**FIG. 7** – Example of graph showing the values of sliding averages ( $M_q$ ) against time (dark blue line) and all the peak-to-peak amplitudes  $A_w$  (yellow line).

results of Test 2 and can rise up to 20% [20]; the BRRC reported them to be up to 3%, with the antennas they tested in the framework of the present research work.

### 3. RESULTS AND DISCUSSION

During 2017, the tests presented in Section 2 were executed in Belgium (BRRC), Czech Republic (University of Pardubice, UP), Portugal (National Laboratory of Civil Engineering, LNEC), and Serbia (Faculty of Technical Sciences of the University of Novi Sad, FTS).

As is resumed in Table I, five commercial impulse control units and nine commercial antennas were tested (five horn antennas and four ground-coupled antennas). One of the FTS antennas was dual-frequency and was tested as two individual antennas, with central frequencies of 400 MHz and 900 MHz. The BRRC and LNEC tested control units are the same model (GSSI SIR 20) and both laboratories tested them with a 1 GHz horn manufactured by GSSI; it is therefore especially interesting to compare the results obtained by BRRC and LNEC on the raw data gathered with the 1 GHz antenna (note that 512 samples per trace were recorded at BRRC, whereas 256 and 1024 samples per trace were recorded at LNEC, with this antenna). All of the tested antennas are

regularly used in fieldwork and none of them had showed signs of malfunctioning before tests were performed.

Note that at LNEC only Tests 1 and 2 were carried out. Note also that the UP team used a smaller metal plate than what is suggested in the tests (see Eq. (1)). Moreover, the UP team carried out Test 3 at different distances between antenna and metal plate than those suggested in the tests (in particular, the UP values were  $h_1=34$  cm,  $h_2=68$  cm and  $h_3=113$  cm); nonetheless, it was decided to include the UP results in this paper.

All obtained results are summarized in Table II.

While performing the tests, it was observed that the maximum amplitude of the direct wave is not always the absolute maximum amplitude of the recorded trace: in most cases, the amplitude of the metal plate reflection is indeed stronger (this is likely due to a reduction of the direct wave implemented by the manufacturers in the tested GPR systems). Furthermore, it was observed that the first collected sample has always a random value, which can be larger than any reflection and shall be discarded.

In Figure 8, results of Tests 1 and 2 obtained on raw and filtered data are compared through histograms; only BRRC and LNEC results are considered in this figure, because FTS and UP always worked with raw data. In most cases, results obtained on filtered data are better than those obtained on raw data. Results obtained for the 1 GHz BRRC antenna are worse than results obtained for all other antennas, including the identical 1 GHz antenna from LNEC, in both Tests 1 and 2, which is an alarm bell on the conditions of the antenna.

In Figure 9, results of Tests 1 and 2 obtained on raw data are compared. Only three antennas show a SNR better than 20. For all antennas, the indicator of the short-term signal stability is higher than 2.8%. Results obtained for the 0.9 GHz UP antenna are significantly worse than results obtained for all other antennas, in both Tests 1 and 2; it is likely that this antenna is not working very well, however it has to be kept in mind that the UP metal plate was too small and this reduces the reliability of the UP results which could be affected by reflections coming from the surrounding environment. The 2 GHz UP antenna shows the highest SNR and not very good value of stability.

TABLE I – TESTED ANTENNAS, SUMMARY.

Institution	Tested GPR control units and antennas	Performed tests	Settings and Remarks
Faculty of Technical Sciences, Novi Sad, Serbia (FTS)	Control unit: GSSI SIR 3000 Ground coupled antennas: GSSI 0.4 GHz GSSI 0.9 GHz  The antennas were purchased in 2003 (0.4 GHz) and 2009 (0.9 GHz). A rough estimate for the number of working hours is 1000 h for the 0.4 GHz antenna and 600 h for the 0.9 GHz antenna.	All tests	- Side length of the metal reflector: 3.5 m (0.4 GHz antenna) and 1.7 m (0.9 GHz antenna). - Samples per trace: 512. - All tests were performed on raw data.
Belgium Road Research Centre, Brussels, Belgium (BRRC)	Control unit: GSSI SIR 20 Horn antennas: GSSI 1 GHz GSSI 2 GHz  All equipment was purchased in 2010. A rough estimate for the working hours of the tested antennas is: 150 h for the 1 GHz antenna, 500 h for the 2 GHz antenna.	All tests	- Side length of the metal reflector: 1.5 m for both antennas. - Samples per trace: 512. - Tests were performed on both raw and filtered data. The applied filters are: - FIR BP 0.25-3 GHz; - FIR BP 0.25-5 GHz; - GSSI NoiseFilter.
University of Pardubice, Pardubice, Czech Republic (UP)	Control units: IDS RIS HiPave, IDS DAD MCH FastWave Ground coupled antennas: IDS 0.4 GHz IDS 0.9 GHz Horn antennas: IDS 2 GHz  All equipment was purchased in 2013. A rough estimate for the total working hours of the tested equipment is 200 h.	All tests	- Side length of the metal reflector: 1 m. - Samples per trace: 512. - All tests performed on raw data.
National Laboratory for Civil Engineering, Lisbon, Portugal (LNEC)	Control unit: GSSI SIR 20 Horn antennas: GSSI 1 GHz GSSI 1.8 GHz  Date of purchase and estimation of working hours not available.	Tests 1, 2	- Rectangular metal reflector, 1 m × 2 m. - Tests performed at 256 and 1024 samples per trace with 1 GHz horn, 512 and 1024 samples per trace with 1.8 GHz horn. - Tests performed on raw and filtered data. The applied filters are: - IIR 0.1-1 GHz; - FIR 0.5-3 GHz; - IIR 0.1-2 GHz; - FIR 0.5-5 GHz.

TABLE II – TEST RESULTS, SUMMARY.

	Antenna	Filter	SNR	Signal Stability	Linearity in time axis	Long Term Stability
1	FTS 0.4 GHz	Raw	10.58	7.91	5.18	2.44
2	FTS 0.9 GHz	Raw	12.48	2.88	2.99	1.57
3	BRRC 1 GHz	Raw	7.24	10.61	4.26	0.92
4	BRRC 1 GHz	FIR	9.70	10.96	3.17	-
5	LNEC 1 GHz	Raw	17.64	5.26	-	-
6	LNEC 1 GHz	FIR-IIR	20.35	2.81	-	-
7	LNEC 1.8 GHz	Raw	15.81	3.89	-	-
8	LNEC 1.8 GHz	FIR-IIR	28.07	1.59	-	-
9	BRRC 2 GHz	Raw	16.21	4.51	6.29	0.69
10	BRRC 2 GHz	FIR	17.45	3.10	3.91	-
11	BRRC 2 GHz	GSSI NF	22.00	2.54	4.56	0.65
12	UP 0.4 GHz	Raw	9.75	4.08	4.88	0.14
13	UP 0.9 GHz	Raw	1.19	15.89	3.39	0.63
14	UP 2 GHz	Raw	23.74	12.18	2.99	1.22

In Figure 10, results of Tests 3 and 4 obtained on raw data are compared. Concerning the linearity in the time axis, the relative variation in the measured speed is always higher than 2.9%. The long-term stability factor is always lower than 3%; the results obtained for the 0.9 GHz UP antenna are worse than those obtained for the other antennas, which may be due to the fact that the antenna is not working well, or to the use of a small metal plate, or else to a scarce accuracy in measuring the distances between metal plate and antenna. Actually, it has been observed by the BRRC research team that results of Test 3 are highly variable and strongly dependent on the laboratory precision; in particular, an error of 1 mm in the measurement of the antenna position can yield an error larger than 2% in the test results. Additionally, it may be appropriate to modify the procedure of Test 3 and use mean values calculated out of, e.g., 100 traces, instead of basing the evaluation of the short-term stability on single waveforms, because of the significant variation of the results that can be observed if measurements are

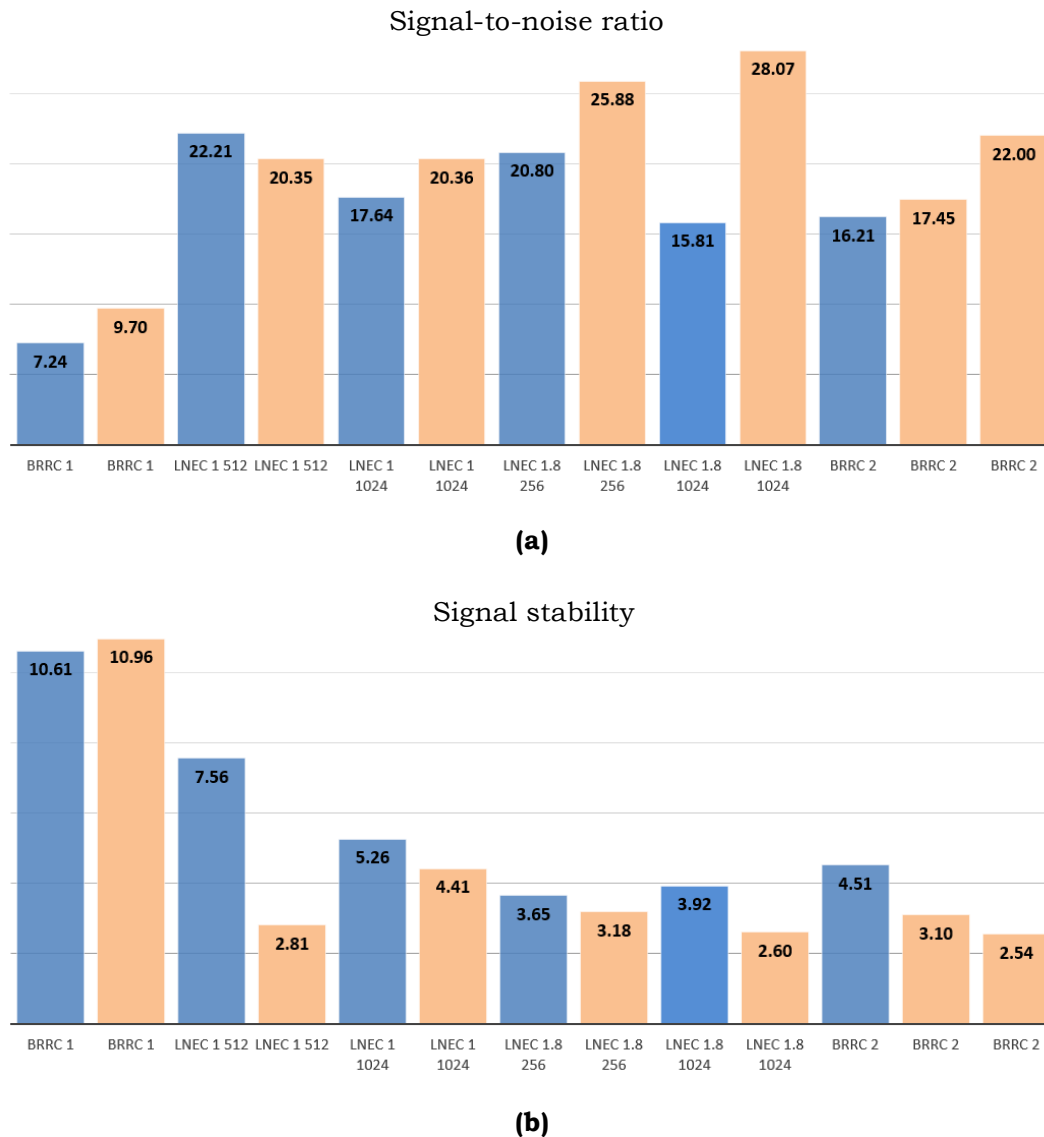
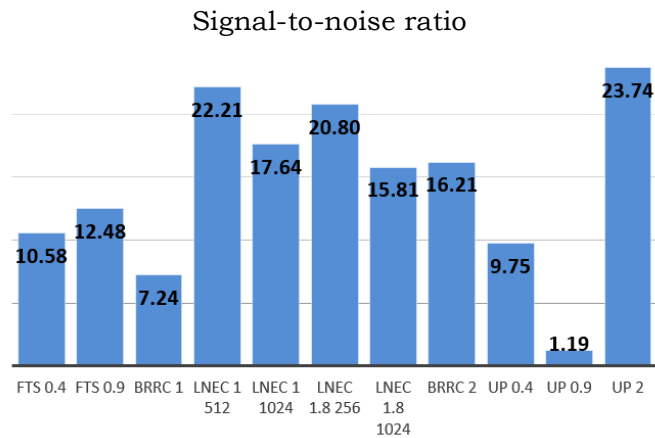
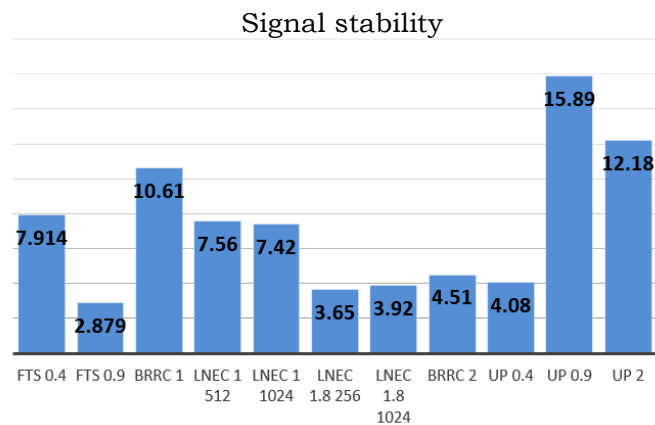


**FIG. 8** - Results of Tests 1 **(a)** and 2 **(b)**, raw and filtered data, BRRC and LNEC only.

repeatedly carried out as suggested in Sub-section 2.3. In particular, the BRRC research team reported that, for a given configuration, the relative variation in the measured speed changed from 0.9% to 17.6%, by repeating the evaluation many times. And so, the BRRC results of Test 3 presented in this paper make already use of mean values calculated out of 100 traces, instead of making use of values calculated out of single traces.



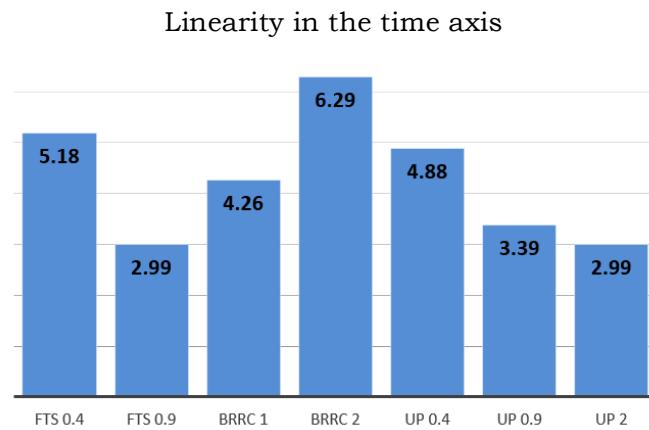
(a)



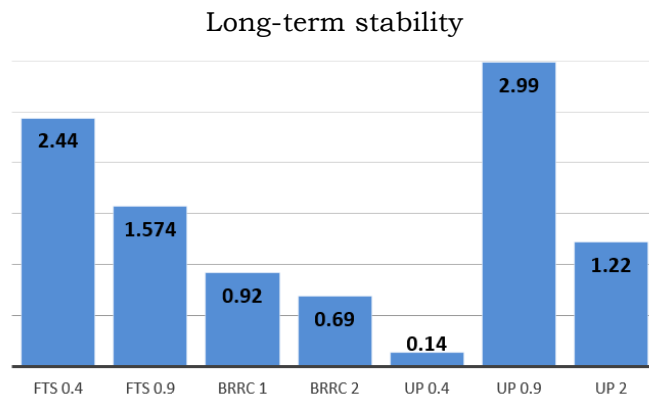
(b)

**FIG. 9** - Results of Tests 1 (a) and 2 (b), raw data only.

Finally, with reference to Test 4, in Figure 11 the sliding averages ( $M_q$ ) are plotted as a function of time for the 2 GHz antenna owned by the BRRC; results in Figure 11(a) were obtained with cold weather and results in (b) were obtained with warm weather. It therefore seems that the results of the tests (and the behaviour of GPR equipment) are strongly affected by the atmospheric conditions; however, more experiments are necessary to confirm this remark and be sure that the weather is the origin of the observed differences.



(a)

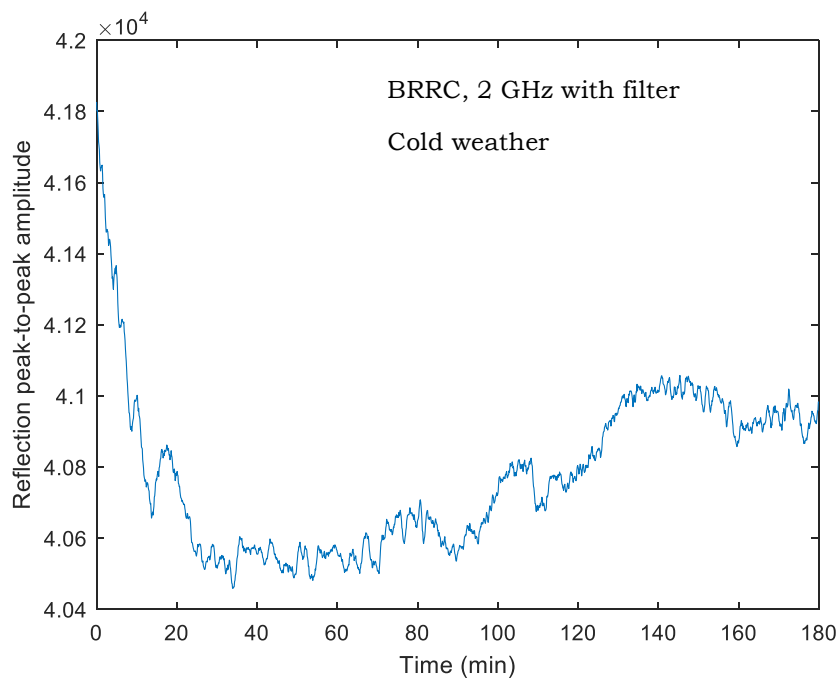


(b)

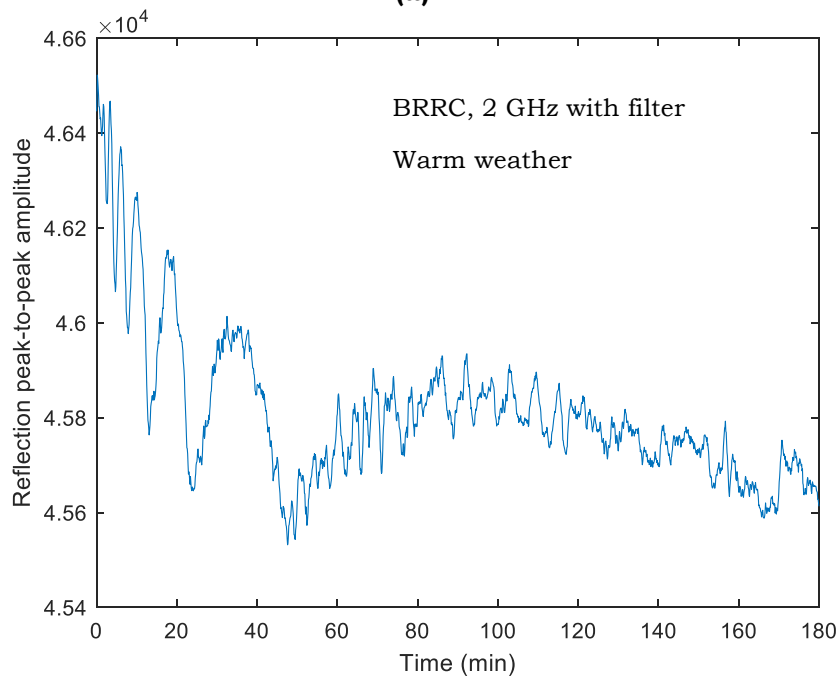
**FIG. 10** - Results of Tests 3 (a) and 4 (b), raw data only.

#### 4. CONCLUSIONS

This paper deals with the design and execution of new experimental tests for assessing the performances of Ground Penetrating Radar (GPR) equipment. After a literature review and a critical analysis of the D6087-08 standard emitted by the American Society for Testing Materials (ASTM International), where typical procedures for the calibration of GPR systems with air-coupled antennas are described, four improved tests were proposed by a team of Members of COST (European Cooperation in Science and Technology) Action TU1208 “Civil engineering applications of Ground Penetrating Radar.” These four tests



(a)



(b)

**FIG. 11** – Test 4, sliding averages of the metal plate reflection peak-to-peak amplitudes ( $M_d$ ) against time. **(a)** Results obtained in cold weather; **(b)** Results obtained in warm weather.

can be carried out to evaluate the signal-to-noise ratio (SNR, Test 1), short-term stability (Test 2), linearity in the time axis (Test 3), and long-term stability of the GPR signal (Test 4); all tests make use of a metal plate and the GPR antenna has to be lifted over it.

Our intention was to keep the procedures simple: we are aware that more accurate tests could be conceived and proposed, however our twofold goal was to propose reliable tests and to foster greater awareness in GPR users of the importance of regularly testing control unit and antennas. Simple procedures ensure that users without a strong scientific background can correctly perform the tests, whereas sophisticated procedures would probably discourage them or be improperly applied.

The paper includes a full description of the four proposed procedures followed by results obtained by research teams from Belgium, Czech Republic, Portugal and Serbia, who performed the tests on commercial GPR systems they own and regularly use in fieldworks. Overall, five pulsed control units and nine antennas were tested (five horn and four ground-coupled antennas, with central frequencies ranging from 400 MHz to 1.8 GHz).

Only three antennas turned out to have a signal-to-noise ratio better than 20. For all antennas, the indicator of the short-term signal stability was higher than 2.8%. Regarding the linearity in the time axis, the relative variation in the measured speed was always higher than 2.9%; in this test, it is crucial to accurately measure the distance between antenna and metal plate and to position the antenna aperture or plane parallel to the ground. The long-term stability factor was always lower than 3%.

The obtained results seem to be fairly consistent: antennas performing well in one test, usually yield good results also in the other tests. The results suggest a malfunctioning of one of the antennas, which performed worse than the other antennas in three tests over four; the low performances of this antennas might be also due to a poor laboratory accuracy in performing the tests and to the metal plate used, which was smaller than suggested.

Based on our tests, a warm-up time of at least 30 min is advised before starting a survey. Our results also suggest that the behaviour of GPR systems may be strongly dependent on atmospheric conditions

(different results were obtained in cold and warm weather), however more experiments are necessary to confirm this observation and better understand the relation between weather and GPR long-term stability.

While the results presented herein are not representative enough to establish absolute thresholds for the tests, they provide a valuable indication about values that one can obtain when testing GPR equipment. At present, we may say that a SNR indicator of at least 10 (20 dB) should be probably obtained when performing Test 1, if the antenna is working well. Reasonably good values of the signal stability indicator (Test 2) should not be larger than 8%. Concerning the linearity in the time axis, the indicator of Test 3 should not be larger than 6.5%. Finally, the long-term signal stability indicator of Test 4 should not be larger than 2.5%. Though reliable thresholds are not yet established, by periodically repeating the tests on the same equipment it is possible to detect shifts from previously obtained values, which may imply that the GPR under test is not working in normal or satisfactory manner. Moreover, the execution of the tests gives stronger awareness about the behaviour and limits of the owned GPR systems.

We hope that other research teams, GPR experts and manufacturers will execute the tests in the near future, on a wider variety of control units and antennas, on both brand new and older equipment, and share the results with the GPR community. In this way, reliable thresholds for the tests can be jointly established and maybe the procedures can be refined and upgraded. It will also be very interesting to investigate how the results of the proposed tests translate into accuracy levels of measured physical and geometrical quantities, in the various applications of the GPR technique. This will allow determining application-specific thresholds, instead of absolute thresholds, as well as thresholds associated with desired accuracy levels of the results.

#### **ACKNOWLEDGEMENTS**

This work was carried out as a contribution to COST (European Cooperation in Science and Technology) Action TU1208 “Civil Engineering Application of Ground Penetrating Radar” ([www.cost.eu](http://www.cost.eu), [www.gpradar.eu](http://www.gpradar.eu)). The authors thank COST for funding and supporting COST Action TU1208.

## REFERENCES

- [1] P. Annan, "GPR—History, Trends, and Future Developments," *Subsurface Sensing Technologies and Applications*, vol. 3, no. 4, pp. 253–270, October 2002, doi: 10.1023/A:1020657129590.
- [2] S. S. Artagan and V. Borecky, "History of using GPR for diagnostics of transport structures," *Proceedings of the 6th International Scientific Conference, Pardubice, Czech Republic, 3–4 September 2015*, 7 pp.
- [3] W. Wai-Lok Lai, X. Dérobert, and P. Annan, "A review of Ground Penetrating Radar application in civil engineering: A 30-year journey from Locating and Testing to Imaging and Diagnosis," *NDT & E International*, vol. 96, pp. 58–78, June 2018, doi: 10.1016/j.ndteint.2017.04.002.
- [4] D. J. Daniels and E. C. Utsi, "GPR case histories and known physical principles," *Proceedings of the 7th International Workshop on Advanced Ground Penetrating Radar (IWAGPR 2013)*, Nantes, France, 2–5 July 2013, pp. 1–9, doi: 10.1109/IWAGPR.2013.6601507.
- [5] E. C. Utsi, "Ground Penetrating Radar: Theory and Practice." Publishing House: Butterworth-Heinemann; Oxford, United Kingdom, April 2017; ISBN: 978008102216; 224 pp.
- [6] A. Benedetto and L. Pajewski, Eds. "Civil Engineering Applications of Ground Penetrating Radar," Publishing House: Springer International; Book Series "Springer Transactions in Civil and Environmental Engineering;" April 2015; e-book ISBN: 9783319048130; hardcover ISBN: 9783319048123; doi: 10.1007/9783319048130; 371 pp.
- [7] X. Núñez-Nieto, M. Solla, P. Gómez-Pérez, and H. Lorenzo "GPR signal characterization for automated landmine and UXO detection based on machine learning techniques," *Remote Sensing*, vol. 6, no. 10, pp. 9729–9748, October 2014, doi:10.3390/rs6109729.
- [8] V. Ferrara, "Technical survey about available technologies for detecting buried people under rubble or avalanches," *WIT Transaction on The Built Environment*, vol. 150, pp. 91-101, May 2015, doi: 10.2495/DMAN150091.
- [9] M. Zajc, B. Celarc, and A. Gosar, "Structural-geological and karst feature investigations of the limestone-flysch thrust-fault contact using low-frequency ground penetrating radar (Adria-Dinarides thrust zone, SW Slovenia)," *Environmental Earth Sciences*, vol. 73, no. 12, pp. 8237-8249, June 2015, doi: 10.1007/s12665-014-3987-x.
- [10] J. Jezova, L. Mertens, and S. Lambot, "Ground-penetrating radar for observing tree trunks and other cylindrical objects," *Construction and*

Building Materials, vol. 123, pp. 214-225, October 2016, doi: 10.1016/j.conbuildmat.2016.07.005.

[11] L. Pajewski, M. Solla, and M. Kuçukdemirci, “Ground-Penetrating Radar for Archaeology and Cultural Heritage Diagnostics: Activities Carried Out in COST Action TU1208,” in: *Nondestructive Techniques for the Assessment of Historic Structures*, L. M. da Silva Goncalves, H. Rodrigues, F. Gaspar, Eds., CRC Press – Taylor & Francis Group, Boca Raton, FL, USA, October 2017, ISBN 9781138710474, pp. 215-225.

[12] J. D. Taylor, Ed., “Advanced Ultrawideband Radar: Signals, Targets, and Applications,” Publishing House: CRC Press – Taylor & Francis Group; Boca Raton, FL, December 2016; ISBN 9781466586574, 494 pp.

[13] A. Zhao, Y. Jiang, and W. Wang, “Signal-to-noise ratio enhancement in multichannel GPR data via the Karhunen-Loève transform,” *Proceedings of the Progress in Electromagnetic Research Symposium*, Hangzhou, China, 22–26 August 2005, vol. 1, no. 6, pp. 754–757, 2005, doi: 10.2529/PIERS041210090705.

[14] X. L. Travassos, D. A. G. Vieira, V. Palade, and A. Nicolas, “Noise reduction in a non-homogenous ground penetrating radar problem by multiobjective neural networks,” *IEEE Transactions on Magnetics*, vol. 45, no. 3, pp. 1454–1457, February 2009, doi: 10.1109/TMAG.2009.2012677.

[15] J. Li, C. Le Bastard, Y. Wang, G. Wei, B. Ma, and M. Sun, “Enhanced GPR signal for layered media time-delay estimation in low-SNR scenario,” *IEEE Geoscience Remote Sensing Letters*, vol. 13, no. 3, pp. 299–303, January 2016, doi: 10.1109/LGRS.2015.2502662.

[16] L. Pajewski and M. Marciniak, “Comparative study of GPR international standards and guidelines,” *Short-Term Scientific Missions - Year 2*, L. Pajewski & M. Marciniak, Eds.; Publishing House: Aracne; Rome, Italy, May 2015; ISBN 978-88-548-8488-5. Available in open access on the website of COST Action TU1208: [www.gpradar.eu/resources/books.html](http://www.gpradar.eu/resources/books.html)

[17] ASTM D6087-08(2015)e1 “Standard Test Method for Evaluating Asphalt-Covered Concrete Bridge Decks Using Ground Penetrating Radar,” ASTM International, West Conshohocken, PA, 2015.

[18] M. R. Mahmoudzadeh Ardekani and S. Lambot, “Full-Wave Calibration of Time- and Frequency-Domain Ground-Penetrating Radar in Far-Field Conditions,” *IEEE Transactions on Geoscience and Remote Sensing*, vol. 52, no. 1, pp. 664–678, January 2014, doi: 10.1109/TGRS.2013.2243458.

[19] L. Mertens, A. P. Tran, and S. Lambot, “Determination of the stability of a pulse GPR system and quantification of the drift effect on soil material characterization by full-wave inversion,” *Proceedings of the 15th International*

Conference on Ground Penetrating Radar (GPR 2014), 30 June – 4 July 2014, Brussels, Belgium, pp. 480–483, doi: 10.1109/ICGPR.2014.6970471.

[20] A. Van der Wielen, “Characterization of thin layers into concrete with Ground Penetrating Radar,” PhD Thesis; Université de Liège, Liège, Belgium, 28 March 2014; 228 pp. (available for free download at <http://hdl.handle.net/2268/163976>, last checked 10 July 2018).

[21] F. I. Rial, H. Lorenzo, A. Novo, and M. Pereira, “Checking the signal stability in GPR systems and antennas,” *IEEE Journal of Selected Topics in Applied Earth Observations and Remote Sensing*, vol. 4(4), pp. 785–790, December 2011, doi: 10.1109/JSTARS.2011.2159779.

[22] T. Scullion, C. L. Lau, and T. Saarenketo, “Performance specifications of ground penetrating radar,” *Proceedings of the 6th International Conference on Ground Penetrating Radar (GPR 1996)*, 30 September–3 October 1996, Sendai, Japan, pp. 341–346.

[23] T. Scullion, C. L. Lau, and Y. Chen, “Implementation of the Texas Ground Penetrating Radar system,” *Interim Report No. FHWA/TX-92/1233-1*, Texas Department of Transportation, November 1992 (revised April 1994), 102 pp.

[24] R. W. Jacob, J. F. Hernance, “Precision GPR measurements: Assessing and compensating for instrument drift,” in *Proceedings of the 10th International Conference on Ground Penetrating Radar (GPR 2004)*, 21–24 June 2004, Delft, The Netherlands, pp. 159–162.

[25] G. Manacorda and M. Miniati, “An easy way of checking impulsive georadar equipment performances,” *Proceedings of the 8th International Conference on Ground Penetrating Radar (GPR 2000)*, 23–26 May 2000, Gold Coast, Australia, 2000, pp. 44–49.

[26] F. Benedetto and F. Tosti, “A signal processing methodology for assessing the performance of ASTM standard test methods for GPR systems,” *Signal Processing*, vol. 132, pp. 327–337, 2017, doi: 10.1016/j.sigpro.2016.06.030.

[27] S. Sebesta, T. Scullion, and T. Saarenketo, “Using Infrared and High-Speed Ground-Penetrating Radar for Uniformity Measurements on New HMA Layers,” *Report No. S2-R06C-RR-1 of the Second Strategic Highway Research Program*, Transportation Research Board of the National Academies, 2013, 81 pp.

[28] D. Goulias and M. Scott, “Effective Implementation of Ground Penetrating Radar (GPR) for Condition Assessment & Monitoring of Critical Infrastructure Components of Bridges and Highways,” *Final Report No. MD-*

15-SHA-UM-3-11, State Highway Administration of Maryland Department of Transportation, January 2015, 173 pp.

[29] R. W. Jacob and J. F. Hermance, "Assessing the precision of GPR velocity and vertical two-way travel time estimates," *Journal of Environmental Engineering and Geophysics*, vol. 9, no. 3, pp. 143–153, September 2004, doi: 10.4133/JEEG9.3.143.

[30] R. W. Jacob and J. F. Hermance, "Random and non-random uncertainties in precision GPR measurements: Identifying and compensating for instrument drift," *Subsurface Sensing Technologies and Applications*, vol. 6, no. 1, pp. 59–71, January 2005, doi: 10.1007/s11220-005-4226-z.

[31] H. Liu, B. Xing, J. Zhu, B. Zhou, F. Wang, X. Xie, and Q. H. Liu, Fellow, "Quantitative Stability Analysis of Ground Penetrating Radar Systems," *IEEE Geoscience and Remote Sensing Letters*, vol. 15, no. 4, April 2018, pp. 522–526, doi: 10.1109/LGRS.2018.2801827.

[32] Webpage of the Final Conference of COST Action TU1208 "Civil engineering applications of Ground Penetrating Radar" (Warsaw, Poland, 25–27 September 2017): [www.gpradar.eu/events-dissemination/conferences/finalconference.html](http://www.gpradar.eu/events-dissemination/conferences/finalconference.html)

[33] M. Vrtunski, L. Pajewski, X. Derobert, Ž. Bugarinović, A. Ristić, M. Govedarica, "GPR antenna testing based on COST Action TU1208 guidelines," *Geophysical Research Abstracts*, European Geosciences Union (EGU) General Assembly 2017, 8–13 April 2018, Vienna, Austria, article ID EGU2018-2353, p. 1.

[34] R. Persico, A. Provenzano, C. Trela, M. Sato, K. Takahashi, S. Arcone, S. Koppenjan, L. G. Stolarczyk, E. C. Utsi, S. Ebihara, K. Wada, E. Pettinelli, L. Pajewski, "Recommendations for the Safety of People and Instruments in Ground-Penetrating Radar and Near-surface Geophysical Prospecting." Publishing House: EAGE Publications bv; Houten, The Netherlands, June 2015, ISBN 9789462821620, 68 pp.

[35] A. Balanis, "Antenna Theory: Analysis and Design," IV edition. Publishing House: John Wiley & sons Inc; Hoboken, NJ, January 2016, ISBN: 9781118642061, 1072 pp.

[36] ASTM D4748–10(2015) "Standard Test Method for Determining the Thickness of Bound Pavement Layers Using Short-Pulse Radar," ASTM International, West Conshohocken, PA, 2015.

The scientific paper that you have downloaded is included in Issue 2, Volume 1 (July 2018) of the journal *Ground Penetrating Radar* (ISSN 2533-3100; journal homepage: [www.gpradar.eu/journal](http://www.gpradar.eu/journal)).

All *Ground Penetrating Radar* papers are processed and published in true open access, free to both Authors and Readers, thanks to the generous support of TU1208 GPR Association and to the voluntary efforts of the journal Editorial Board. The publication of Issue 2, Volume 1 is also supported by Adapis Georadar Teknik Ab ([georadar.eu](http://georadar.eu)) and by IDS Georadar s.r.l. ([idsgeoradar.com](http://idsgeoradar.com)).

The present information sheet is obviously not part of the scientific paper.

